




13.8%


Date: 2024-08-25 09:38 UTC


* All sources 100 | Internet sources 10 | Plagiarism Prevention Pool 47


- [31]  from a PlagScan document dated 2021-07-26 12:01
1.8% 27 matches
 1 documents with identical matches


- [37]  from a PlagScan document dated 2022-02-16 04:52
1.3% 21 matches


- [39]  from a PlagScan document dated 2022-09-26 06:30
1.3% 19 matches


- [44]  www.ncbi.nlm.nih.gov/pmc/articles/PMC9000705/
1.1% 18 matches


- [45]  from a PlagScan document dated 2022-10-09 08:20
1.5% 20 matches


- [49]  from a PlagScan document dated 2021-11-29 08:30
1.2% 15 matches

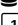
- [50]  from a PlagScan document dated 2021-11-04 06:55
1.2% 15 matches

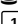
- [51]  from a PlagScan document dated 2021-08-27 09:01
1.1% 15 matches

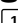
- [52]  from a PlagScan document dated 2021-04-18 08:46
1.3% 18 matches

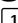
- [53]  from a PlagScan document dated 2021-12-09 13:03
1.2% 18 matches

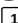
- [54]  from a PlagScan document dated 2018-03-12 06:34
1.2% 14 matches

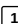
- [55]  from a PlagScan document dated 2018-02-19 10:24
1.3% 16 matches

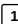
- [56]  from a PlagScan document dated 2019-12-03 12:56
1.1% 16 matches

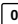
- [57]  from a PlagScan document dated 2017-10-06 15:30
1.0% 14 matches

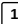
- [58]  from a PlagScan document dated 2022-06-28 08:49
1.1% 15 matches

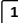
- [59]  from a PlagScan document dated 2022-05-01 07:40
1.0% 17 matches

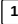
- [60]  from a PlagScan document dated 2015-12-01 11:13
1.0% 14 matches

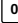
- [61]  from a PlagScan document dated 2022-04-29 16:43
1.1% 16 matches

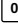
- [62]  from a PlagScan document dated 2021-10-09 14:30
0.9% 12 matches


- [63]  www.ncbi.nlm.nih.gov/pmc/articles/PMC11247902/
1.1% 13 matches






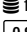

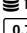
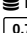

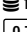
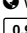
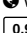
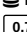
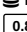
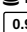
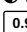
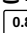
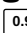
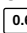
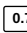
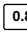
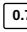
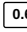
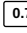
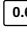
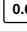

- [64]  www.frontiersin.org/journals/pharmacology/articles/10.3389/fphar.2021.809308/full
1.1% 11 matches


- [65]  from a PlagScan document dated 2023-03-10 06:23
1.0% 18 matches


- [66]  from a PlagScan document dated 2022-06-27 09:41
0.9% 14 matches


- [67]  from a PlagScan document dated 2020-08-28 17:06
0.8% 11 matches
 1 documents with identical matches


- [69]  www.ncbi.nlm.nih.gov/pmc/articles/PMC7866537/
1.0% 14 matches


-
- [70]  from a PlagScan document dated 2022-12-01 09:23
0.9% 10 matches
-
- [71]  from a PlagScan document dated 2018-09-23 21:01
0.8% 9 matches
-
- [72]  from a PlagScan document dated 2018-01-29 07:08
1.0% 13 matches
-
- [73]  from a PlagScan document dated 2022-06-13 16:18
0.8% 12 matches
-
- [74]  from a PlagScan document dated 2018-04-10 07:00
0.9% 9 matches
-
- [75]  from a PlagScan document dated 2022-06-28 09:01
0.9% 13 matches
-
- [76]  from a PlagScan document dated 2019-07-17 08:19
0.7% 10 matches
-
- [77]  from a PlagScan document dated 2021-11-01 12:03
0.7% 11 matches
-
- [78]  from a PlagScan document dated 2019-01-22 20:05
0.7% 13 matches
1 documents with identical matches
-
- [80]  from a PlagScan document dated 2020-06-30 08:30
0.8% 13 matches
-
- [81]  from a PlagScan document dated 2023-04-27 09:47
0.7% 10 matches
-
- [82]  www.researchgate.net/publication/303585246_Anabolic_therapy_with_Euiseum_arvense_along_with_bone_mineralising_nutrients_in_ovari
0.9% 11 matches
-
- [83]  www.ncbi.nlm.nih.gov/pmc/articles/PMC5943608/
0.9% 10 matches
-
- [84]  from a PlagScan document dated 2022-04-30 04:16
0.7% 11 matches
-
- [85]  from a PlagScan document dated 2022-06-15 08:51
0.8% 11 matches
-
- [86]  from a PlagScan document dated 2022-03-31 07:52
0.9% 11 matches
-
- [87]  www.ncbi.nlm.nih.gov/pmc/articles/PMC11087471/
0.9% 10 matches
-
- [88]  from a PlagScan document dated 2020-07-09 10:28
0.8% 12 matches
-
- [89]  from a PlagScan document dated 2018-03-15 10:56
0.9% 12 matches
-
- [90]  www.ncbi.nlm.nih.gov/pmc/articles/PMC6526636/
0.6% 9 matches
-
- [91]  from a PlagScan document dated 2022-05-05 17:35
0.7% 10 matches
-
- [92]  www.nature.com/articles/s41418-017-0020-4
0.8% 8 matches
-
- [93]  from a PlagScan document dated 2018-04-03 03:40
0.7% 8 matches
-
- [94]  from a PlagScan document dated 2022-05-17 08:26
0.6% 10 matches
-
- [95]  from a PlagScan document dated 2019-07-08 16:25
0.7% 11 matches
-
- [96]  from a PlagScan document dated 2022-04-28 06:29
0.6% 12 matches
-
- [97]  from a PlagScan document dated 2023-11-29 11:09
0.6% 7 matches
-
- [98]  from a PlagScan document dated 2022-06-15 08:51
0.8% 11 matches

- ✓ [98]  from a PlagScan document dated 2022-06-13 08:51
0.7% 13 matches


- ✓ [99]  from a PlagScan document dated 2021-11-24 10:50
0.5% 8 matches

- ✓ [100]  from a PlagScan document dated 2022-04-29 16:43
0.6% 7 matches

- ✓ [101]  from a PlagScan document dated 2019-11-18 10:22
0.6% 10 matches

- ✓ [102]  www.ncbi.nlm.nih.gov/pmc/articles/PMC7783214/
0.6% 10 matches

23 pages, 6218 words

 The document contains a suspicious mixture of alphabets. This could be an attempt of cheating.

PlagLevel: 13.8% selected / 22.9% overall

183 matches from 103 sources, of which 18 are online sources.

Settings

Data policy: *Compare with web sources, Check against my documents, Check against the Plagiarism Prevention Pool*

Sensitivity: *High*

Bibliography: *Bibliography excluded*

Citation detection: *Highlighting only*

Whitelist: *--*

1 Quercetin has a protective impact on human umbilical vein endothelial cells against
2 tungsten carbide cobalt nanoparticle-induced cytotoxicity, oxidative stress,
3 apoptosis

4

5 Abstract

6 Oxidative stress is a pivotal factor in the pathogenesis of various cancer diseases.^[89] In fact,
7 oxidative DNA damage is described as the type of damage probably to occur in cancer
8 cells.^[89] This study examined the protective impact of the polyphenolic compound quercetin
9 on human umbilical vein endothelial (HUVEC) cells against tungsten carbide cobalt
10 nanoparticles (WC-Co NPs)-induced oxidative stress, cytotoxicity, and apoptosis.^[31] One of
11 the most often used models for studying endothelial cells in vitro is the human umbilical
12 vein epithelial cell.^[89] Scanning electron microscope (SEM) and transmission electron
13 microscopy (TEM) were used to measure the size of the NPs prior to WC-Co NPs
14 treatment. WC-Co NPs had a polygonal form and measured 45.26 ± 1 nm in size.^[70] Using
15 3-(4,5-dimethylthiazol-2-yl)-2,5-diphenyltetrazolium bromide (MTT),^[52] neutral red
16 uptake (NRU) and lactate dehydrogenase (LDH) assays, the cytotoxicity of WC-Co NPs
17 on HUVECs cells was assessed.^[75] The cytotoxicity of NPs increased in a concentration-
18 dependent way.^[52] The MTT result was used to calculate the median inhibitory
19 concentration (IC₅₀) for HUVEC cells at 24 hours, which came out to be 23.14 µg/ml.
20 Intracellular reactive oxygen species (ROS) and lipid peroxidation (LPO) levels were
21 elevated at 17 g/ml WC-Co NPs and then reduced in HUVECs cells upon immediate
22 exposure to 150 µM quercetin (QR).^[39] Using JC-1 staining, the loss of mitochondrial
23 membrane potential (MMP) in control, WC-Co NPs alone and WC-Co NPs plus QR
24 exposed cell were evaluated.^[44] In HUVECs cells, maximum apoptotic cells were seen at

25increasing NPs concentrations. ^[97]Based on the impacts of NPs on HUVECs cells, the data
26suggests that QR may work on the process of scavenging ROS, which is responsible for
27DNA repair. ^[97]Consequently, the above findings highlight the significance of these QR as
28defenses against DNA damage brought on by oxidative stress, which frequently happens
29in a number of cancer disorders.

30Keywords: Tungsten carbide cobalt nanoparticle; ROS; HUVECs cells; Apoptosis.

31

32Introduction

33Products based on nanotechnology have been sold and used on humans and living
34animals, including adhesives, medicines, cosmetics, and artificial organs and tissue.
35^[57]Nonetheless, prior reports suggested that these nanomaterials could be used in the
36healthcare industry and/or other fields without risk; ^[51]therefore, it is important to
37thoroughly assess their toxicity. ^[71]Research is still being conducted to validate the safety
38and exposure route of nanoparticles. ^[57]Because of the disparity in sizes, there is particular
39debate regarding the toxicity of nanoscale materials. ^[101]However, recently, there has been
40growing interest in the use of bimetallic NPs for treatment of contaminated groundwater
41and soils and antimicrobial effects (Kim et al., 2014). Tungsten carbide nanoparticles are
42now being considered for the manufacture of hard metals to achieve extreme hardness
43and wear resistance, and mixing with cobalt is thought to improve toughness and strength
44of the material (Bastian et al., 2009). However, the so-recent report indicated that there
45was a lack of systematic assessment of the DNA damaging and carcinogenic potential of
46bimetallic NPs in spite of their extensive use in nanotechnological applications (Arora et
47al., 2020). ^[72]Based on insufficient data in people and sufficient evidence in experimental

48animals, the International Agency for Research on Cancer has officially classed the hard
49metal tungsten carbide as potentially carcinogenic to humans (IARC 2006).

50^[74] Human umbilical vein endothelial cells, or HUVECs, have been a key model system in
51the study of endothelial cell function regulation and the function of the endothelium in
52the blood vessel wall's response to shear forces, stretch, and the formation of
53atherosclerotic plaques and angiogenesis. In nanotoxicological and/or nanomedicine
54studies, endothelial cells are of particular interests for two main reasons. ^[78] First, it serves as
55the first contact for NPs entering the blood before NPs are delivered to targets (Cao et al.,
562017). ^[95] Therefore, although only some of the NPs are intended to target the blood vessels,
57it has been suggested that the interactions between endothelial cells and NPs should be
58carefully assessed to better understand the potential in vivo effects of NPs (Setyawati et
59al., 2015).

60^[87] Since quercetin affects glutathione, enzymes, signal transduction pathways, and ROS
61generation, it is useful in the treatment and prevention of human diseases. ^[87] According to
62recent research, quercetin's antioxidant properties mostly show up as effects on signal
63transduction pathways, glutathione, enzymatic activity, and reactive oxygen species
64brought on by toxicological and environmental variables. Particle size, content, and
65associated reactivity all affect the toxic effects on human endothelial cells (Mirowsky et
66al., 2013). Experimental study has revealed a larger mutagenesis potential of the WC-Co
67mixture when compared with its individual components, according to van Goethem et al.
68(1997). This finding has been connected to increased ROS production.

69Thus, in this experiment, we examined the cytotoxicity and apoptotic characteristics of
70WC-Co NPs on 24-hr-on HUVEC cells. NPs mediated toxicity involves various

71 mechanisms, specifically, the over production of ROS in living tissue under stress.^[51] Cells
72 primarily produce reactive oxygen species from mitochondria, and the electron transport
73 chain is where most of the ROS is produced. Oxidative stress, apoptotic responses and
74 genotoxicity reactions are the principal mechanisms of toxicity in WC-Co NPs.^[73] The
75 objective of this study was to investigate the toxic effects of WC-Co NPs on HUVECs
76 cells.^[82] Furthermore, our results will be useful in assessing the environmental friendliness
77 and safety of WC-Co NP use in industry.

78 ^[66] 2. Materials and Methods

79 2.1. Chemicals and Reagents

80 The chemicals such as quercetin ($\geq 95\%$ (HPLC grade, cat no. Q4951),^[55] 4,5-dimethyl-2-
81 thiazolyl)-2,5 diphenyl-2H-tetrazolium bromide (MTT), Dimethyl sulfoxide (DMSO),
82 Hoechst 33258 fluorescent dye, 2',7'-dichlorodihydrofluorescein diacetate (H2DCFDA),
83 Dulbecco's Modified Eagle Medium (DMEM), Phosphate Buffered Saline (PBS), Fetal
84 Bovine Serum (FBS), Trypsin- EDTA solution 1x etc.^[37] were purchased from Sigma-
85 Aldrich. From US Research Nanomaterial Inc., tungsten carbide cobalt nanopowder
86 (WC/Co)-Co-5wt%,99%,40-80nm was acquired.^[88] Other chemicals related to the current
87 experiment were bought at local markets.

88 2.2. Physicochemical characterization of tungsten carbide cobalt nanoparticle (WC-Co 89 NPs)

90 The physical characterization of WC-Co NPs was done by SEM and TEM (JEOL Inc.,
91 Tokyo, Japan). We have determined the size of WC-Co NPs in water by using dynamic
92 light scattering instruments (Malvern, UK). Using an X-ray source of (CuK α , $\lambda =$

930.15406 nm) radiations as a Ni filter, a PANalytical X'Pert X-ray diffractometer was used
94to record the powder X-ray diffraction pattern of WC-Co nano powder.

952.3. Cell culture

96 Human umbilical vein endothelial (HUVECs) cell lines were purchased from an
97American type culture collection (Manassas, VA, USA) and its accession no. is ATCC
98No. CRL-17305^[83]. Cells were grown in Dulbecco's modification of eagle's medium
99(DMEM), supplemented with 10% fetal bovine serum (FBS) and 1% antibiotic, cells
100were maintained in a CO₂ (5%) incubator at 37°C.

1012.4. Exposure of WC-Co NPs and QR

102WC-Co NPs were suspended in a cell culture medium and diluted to appropriate
103concentrations (0, 5, 10, 25, 50, 100, and 150 µg/ml) to treatment for 24 h. The
104appropriate dilutions of WC-Co NPs were then sonicated using a sonicator probe. The
105following treated cells were harvested to determine cytotoxicity, oxidative stress,
106apoptotic, proinflammatory responses, and gene expression. Cells not exposed to WC-Co
107NPs served as a control in each experiment. The QR (150 µM) was used as a protective
108effect against WC-Co NPs toxicity on HUVECs cells for 24 h.

1092.5. ^[58] MTT assay and determination of IC₅₀ 24 h of WC-Co NPs and QR

110The MTT assay was used to investigate mitochondrial function as described by Mossman
111(Mossman, 1983). ^[58] HUVECs cells were seeded into a 96-well plate (8 × 10⁴ cells/well) in
112the complete medium at the volume of 100 µl/well. ^[80] After overnight incubation, the
113medium was removed and 100 µL growth culture containing a series of different
114concentrations of WC-Co NPs (0, 5, 10, 25, 50, 100, and 150 µg/ml) at 24 hr. ^[77] The

115medium was replaced by MTT solution (5 mg/ml), at a volume of 20 μ L to each well and
116incubated for 4 h at 37°C in a dark.^[55] After incubation, the MTT solution was removed, and
117formazan crystals formed by mitochondrial reduction of MTT were solubilized in (100 μ L/
118well) DMSO and gently shaken for 15 minutes.^[31] The plates were read using a microplate
119reader (Synergy-H1; BioTek) at a wavelength of 570 nm.^[31] The assay was performed in
120triplicate with four replicates per sample.^[54] The survival rate of the cells was calculated
121using the following formula:

122^[31] Cell viability rate (%) = Optical Density (OD) values of the treated samples /OD value of
123control *100.

124^[49] Based on the IC₅₀-24 h value, the three test concentrations of WC-Co NPs were
125calculated viz., concentration I (1/4th of LC₅₀ = ~ 6 μ g/ml), concentration II (1/2nd of
126LC₅₀ = ~ 11 μ g/ml) and concentration III (3/4th of LC₅₀ = ~ 17 μ g/ml).^[49] After establishing
127the IC₅₀ values for WC-Co NPs alone and 150 μ M quercetin was used as a protective
128effect against WC-Co NPs toxicity on HUVECs cells.

1292.6.^[58] Neutral Red Uptake (NRU) Assay

130The lysosomal activity was measured by the NRU assay according to the method of Ali
131et al., (2010).^[54]

132The cytotoxicity rate of the cells was calculated using the following formula:

133Cytotoxicity (%) = (OD in control cells - OD in treated cells)/(OD in control cells)*100 .

1342.7.^[44] LDH assay

135The release of cytoplasmic LDH enzyme into the culture, the medium was determined
136(Ali et al., 2011).^[98] The rate of NADH oxidation was determined by the absorbance was
137measured at 490 nm using a spectrophotometric microtiter plate reader (Synergy-H1;
138BioTek) and was calculated using this formula: Cytotoxicity (%) = (Test sample- Low
139control)/(High control-Low control)*100.

1402.8.^[100] Measurement of intracellular reactive oxygen species

141Reactive oxygen species (ROS) generation was assessed in HUVECs cells after exposure
142to different concentrations by using 2,7-dichlorofluorescein diacetate (DCFH-DA) dye as
143a fluorescence agent based on the method demonstrated. ROS generation was studied by
144two methods: fluorometric analysis and microscopic fluorescence imaging.^[50] For
145fluorometric analysis, cells (7×10^4 per well) were seeded in 96-well black bottom
146culture plates and allowed to adhere them for 24 h in a CO₂ incubator at 37C.^[85] After
147discarding the old medium, the HUVECs cells were incubated in the medium containing
148various concentrations (Control, QR 150µM alone, 6 µg/ml, 11µg/ml, 17µg/ml of WC-
149Co NPs and 17µg/ml of WC-Co NPs + QR) for 24 hr.^[50] On the completion of respective
150exposure periods, cells were incubated with pre-prepared 1X DCFH-DA (10 mM) by
151adding µL of dye solution to 99µL of DMEM in dark for 60 min at 37C.^[50] The reaction
152mixture was aspirated and replaced by 200 µL of PBS in each well.^[31] The plates were kept
153in a shaker for 10 min at room temperature in the dark.^[31] Fluorescence intensity was
154measured using a microplate reader at excitation wavelength 485 nm and at emission
155wavelength 535 nm and values were expressed as a percent of fluorescence intensity
156relative to control wells.^[44] A parallel set of cells (7×10^4 per well) was analyzed for

157intracellular fluorescence using an upright fluorescence microscope equipped with CCD
158cool camera (Nikon Eclipse 80i equipped with Nikon DS-Ri1 12.7-megapixel camera).

159 2.9. Oxidative stress biomarkers

160 HUVECs cells were seeded in 25 cm² culture flasks at a concentration of (5×10^5 /flask)
161and incubated at 37° and exposed with (Control, QR 150µM alone, 6 µg/ml, 11µg/ml,
16217µg/ml of WC-Co NPs and 17µg/ml of WC-Co NPs + QR) for 24 hr.^[99] Next, cells were
163rinsed **three times with** cold PBS and buffer solution was added according to each assay
164protocol and scraped by scraper (Fisher Brand Cell scrapers, Fisher Scientific, USA) and
165collected in a glass tube after scraping.^[90] Then, the cell suspension was sonicated **for 10**
166**min at 4°C** by a Q700 sonicator.^[90] After sonication, lysis buffer was mixed in scrapped
167cells **and centrifuged at** 4500 rpm for 15 minutes at 4C and the supernatant (cell lysate)
168was put on ice to determine CAT activity and LPO.

169 2.9.1.^[45] Measurement of catalase level

170The CAT activity **was determined using the** commercially available enzyme assay kit
171Cayman's.^[50] **According to the manufacturer's** protocol.^[45] Absorbance was read at 540 nm
172**using a microplate reader** (Synergy-H1; BioTek).

173 2.9.2.^[88] Measurement of LPO level

174The extent of membrane LPO **was estimated by measuring the formation of**
175malondialdehyde (MDA) using the 'Cayman's lipid hydroperoxide experiment kit'.
176^[45] **According to the manufacturer.**^[31] absorbance was read at 500 nm **using a microplate reader**
177(Synergy-H1; BioTek).

178 2.10.^[64] Determination of MMP

179The fluorescence dye 5,5',6,6'-tetrachloro-1,1',3,3'-tetraethylbenzimi-
180dazolylcarbocyanine iodide (JC-1) was used to evaluate the effect of compounds on the
181potential permeabilization of the mitochondrial membrane in HUVECs cells.^[52] MMP was
182determined using the commercially available enzyme assay kit Cayman's.^[54] According to
183the manufacturer's protocol.

1842.11. Assessment of gene expression using q RT-PCR

1852.11.1. RNA extraction^[59]

186The cells were seeded in T-25 flask at a density of 5×10^6 cells/ flask for 24 hr at 37°C in
187CO₂ incubator.^[52] At 80-90 % confluence, the cells were exposed to different concentrations
188of WC-Co nanoparticles and QR as follows (150 µM QR, 6 µg/ml, 11µg/ml, 17µg/ml of
189WC-Co NPs, 17µg/ml WC-Co NPs + 150 µM QR) for 24 hr.^[60] After 24 hr of incubation
190media were removed and cells were then rinsed twice with cold PBS and then harvested
191by adding 800 µl of TRIzol™ Reagent (cat no. 15596026, Thermo Fisher) directly in
192each flask the flask was incubated on ice for 5 minutes.^[91] Next, the cell lysate was then
193transferred to a 1.5 ml Eppendorf tube, and 200 µl of cold chloroform was added to the
194tube for phase separation.^[91] After that, the tube was gently shaken by hand for 10 seconds.
195The tube was then centrifuged at 4200 RCF for 15 min at 4°C.^[59] After centrifugation, the
196upper aqueous phase containing total RNA was transferred to a new tube.^[90] For RNA
197precipitation, 500 µl of isopropyl alcohol was added, and were kept on ice for 10 min
198before being centrifuged at 4200 RCF for 10 min at 4°C.^[78] The supernatant was then
199carefully removed, leaving a white gel-like pellet containing RNA attached to the bottom
200of the tube.^[76] The RNA pellet was rinsed with 1000 µl of cold absolute ethanol and
201centrifuged at 3500 RCF for 5 min at 4°C.^[63] Thereafter, the supernatant was discarded, and
202the RNA pellet was air-dried for 10 min.^[31] After, 22 µl of DEPC-treated water was added
203to the tube.^[60] The RNA concentration and purity were measured using a Nanodrop 8000
204spectrophotometer. The RNA purity absorbance ratio (260 A / 280 A = 1.5-2) and the
205contamination and precipitation absorbance ratios (260 A / 230 A = 1.5-2).

206 2.11.2. cDNA synthesis

207 After determining the quantity and purity of RNA, a high-capacity cDNA reverse
 208 transcriptase kit (Cat. No. 4368814, Thermo Fisher Scientific, USA) was used to create
 209 cDNA from 1000 ng/ μ l of each RNA sample. All cDNA preparation steps were
 210 performed on ice.

211 ^[39] The preparation of the cDNA reverse transcription reaction was done by carefully mixing
 212 10 μ l of reverse transcription master mix with 10 μ l of diluted RNA samples into
 213 microcentrifuge tubes and placed in a Thermal cycler (TECHNE, UK); ^[39] according to the
 214 technique listed in Table 1. Then, cDNA was diluted with 180 μ l nuclease-free water or
 215 DEPC and kept at 4°C.

216 Table 1. Thermal cycler conditions

	Step 1	Step 2	Step 3	Step 4
Temperature (°C)	25	37	85	4
Time	10 min	120 min	5 min	∞

217

218 Small amounts of the cDNA sequences were amplified exponentially throughout a series
 219 of temperature changes using PCR techniques, and the resulting copies were then kept at
 220 4°C. Agarose gel electrophoresis was used to validate the presence of cDNA in the
 221 samples. By passing the charged molecules through an agarose matrix with the help of an
 222 electric field, the cDNA fragments were divided into different sizes.

223 2.11.3. Quantification of mRNA expression by qRT-PCR

224 Quantification analysis of reference gene, GAPDH, and apoptosis-associated genes
 225 (caspase-3, p53, Bax, Bcl2) was performed by real-time RT-PCR. On the ice, a reaction
 226 mixture was prepared as per Table 2. First, 17.5 μ l of the reaction mixture was pipetted
 227 into the wells of a 96-well PCR plate. Then, 2.5 μ l of cDNA ^[95] was added to the wells to
 228 contain a total reaction volume of 20 μ l. The reaction plate was sealed and centrifuged
 229 into the real-time PCR instrument (Prime Q). Afterward, the plate was analyzed by
 230 Techne® Prime Q, a Real-time PCR System. ^[31] Table 3 shows the primer sequence for the
 231 genes. ^[95] To obtain more accurate results, all samples were run in duplicate.

232 Table 2.^[95] The contents of the RT-PCR master mix for each gene preparation

Component	Volume needed per sample (ul)
GoTaq qPCR Master Mix (syber green 2x)	10µl
Primers reverse, forward	1.6µl
DEPC water	11.9µl
cDNA Sample	2.5µl
Total per reaction	20µl

234 Table 3. The sequences of primers

Gene	Forward	Reverse	Size(bp)
Bax	5'-ATGTTTTCTGACGGCAACTTC-3'	5'-AGTCCAATGTCCAGCCCAT-3'	134
Bcl-2	5'-ATGTGTGTGGAGACCGTCAA-3'	5'-GCCGTACAGTCCACAAAGG-3'	195
p53	5'-AGAGTCTATAGGCCACCCC-3'	5'-GCTCGACGCTAGGATCTGAC-3'	882
Caspase-3	5'-TGTTTGTGTGCTTCTGAGCC-3'	5'-CACGCCATGTCATCATCAAC-3'	125
GAPDH	5'-CTTTTGCCTCGCCAGGTGAA-3'	5'-AGGCGCCCAATACGACCAAA-3'	189

235

236

237 The comparative threshold cycle ($2^{-\Delta\Delta CT}$) approach was utilized to evaluate the mRNA

238 abundance (Laila et al., 2020). Every sample was measured using a minimum of two

239 independent experiments, and the comparison analysis's mean \pm SE is used to express the

240 results.

241

242 2.12. Analysis of Data

243 Statistical analysis was performed by GraphPad Prism Software (version 8.0.^[31], La Jolla

244 California USA) using one-way ANOVA, followed by post hoc Tukey's multiple

245 comparison tests, as suggested by the software.^[80] Data were shown as mean \pm SE of at least246 three independent experiments.^[101] Differences were considered significant at $p < .05$ (*); p

247.01 (**), p ^[66].001 (***), and p .0001 (****). Minimum 3 independent experiments
248 were done in duplicate for each experiment.

2493. Results

2503.1 Physical characterization of WC-Co NPs

251 SEM-EDS results confirmed the presence of tungsten, carbon, cobalt in NPs and of other
252 elements (Fig. 1A, B). Such as C at 0.15 keV, W at 2.12 keV and Co at 6.840 to confirm
253 the formation of WC-Co nanoparticles (Figure 1A). The typical size of WC-Co NPs is
254 45.26 ± 1 nm (Fig. 1C). The production of WC-Co NPs is confirmed by the XRD result
255 (Fig. 1D).

256 ^[93]DLS and zeta potentials were used to measure the particle size and stability of WC-Co
257 NPs in suspension. ^[93]The size of WC-Co NPs was measured at 180 ± 5 nm zeta potential on
258 the surface of the NPs in aqueous solution were measured by -0.952 mV.

2593.2. IC₅₀ value of WC-Co NPs on HUVECs cells

260 The IC₅₀ value 24 hr for WC-Co NPs on HUVECs cells were determined by the dose-response
261 curve graph using the program Origen Pro 8.5 (Fig. ^[39]2) and it was determined on the basis of the
262 MTT test result. We observed that IC₅₀ value at 24 hr for NPs was 23.114 µg/ml for HUVECs
263 cells (Figure 2).

2643.3. ^[31]Cytotoxicity of WC-Co NPs on HUVECs cells

265 Total cell viability is proportional to the number of viable cells, which are metabolically
266 active cells that convert the tetrazolium salt (MTT) to a purple formazan crystal. ^[53]The
267 different concentrations of WC-Co NPs (0, 5, 10, 25, 50, 100, and 150 µg/ml) were
268 exposed to HUVECs cells for 24 hr. ^[53]The results revealed a significant increase in cell

269toxicity in the HUVECs cells (0%, 31.4%, 43.6%, 47.8%, 58%, 65%, 79.8%) (Figure
2703A).

271^[58] The NRU assay results for HUVECs cells show that NPs caused cytotoxicity in a
272concentration-dependent manner (Figure 2B).^[58] The results indicated an increase in cell
273toxicity with (0%, 14%, 22%, 26%, 29%, 34.6%, 42%) for HUVECs cells (Fig. 3B).

274The leakage of lactate dehydrogenase (LDH) enzyme in HUVECs cells was maximum at
27517 µg/ml of WC-Co NPs and it was decreased 200% due to effect of QR exposure (Fig.
2763C).

2773.4.^[55] Reactive oxygen species (ROS)

278The production of reactive oxygen species (ROS) was measured using the 2', 7-
279dichlorofluoresceindiacetate (DCFH-DA) dye as a fluorescence agent.^[72] In brief, different
280concentrations such as (0 µg/ml, Quercetin150 µM, 6 µg/ml NPs, 11 µg/ml NPs, 17 µg/ml
281NPs and 17 µg/ml NPs followed by Quercetin150 µM were exposed to HUVECs cells for
28224 hr, and then an ROS assay was performed.^[66] The result shows an increasing effect of
283reactive oxygen species in treated cells compared to control (100%, 120%, 138%, 142%,
284156% and 137%) for cells, (Fig. 4A). The scavenging effect of QR was observed in
285decrease in ROS production at 17 µg/ml NPs followed by Quercetin150 µM QR. Fig.4B
286shows ROS expression in HUVECs cells.

2873.5. Oxidative stress assay

288The results indicate an increase in LPO activity for treated cells compared to non-treated
289control cells in HUVECs cells. The LPO activity was found as 100 % for control, 140%

290for Quercetin150 μ M, 150% for 6 μ g/ml NPs, 160% for 11 μ g/ml NPs, 198 % for 17 μ g/
291ml NPs and 170% for 17 μ g/ml NPs followed by Quercetin150 μ M were exposed to
292HUVECs cells (Fig.5A).

293The results revealed a decrease in CAT activity as16 nm/ml/mn for control, 14 nm/ml/mn
294for Quercetin150 μ M, 10 nm/ml/mn for 6 μ g/ml NPs, 9.5 nm/ml/mn for 11 μ g/ml NPs,
2958.2 nm/ml/mn for 17 μ g/ml NPs and 10.4 nm/ml/mn for 17 μ g/ml NPs followed by
296Quercetin150 μ M were exposed to HUVECs cells (Fig.5B).

2973.8.^[72] Measurement of MMP in HUVECs cells

298 Using a confocal microscope to find apoptotic cells based on **mitochondrial membrane**
299**potential** loss detected with JC-1 dye that appear as green (apoptotic) and red (healthy
300cells) Cells were seeded at a density of 8×10^4 in 200 μ l of culture medium in transparent
3016-well plates and exposed to (0 μ g/ml, Quercetin150 μ M, 6 μ g/ml NPs,11 μ g/ml NPs, 17
302 μ g/ml NPs and 17 μ g/ml NPs followed by Quercetin150 μ M **were exposed to** HUVECs
303cells for 24 hr,.^[70] Results **showed a significant increase in the number of apoptotic cells**
304**compared to the control** untreated cells in cell line.^[70] NPs treatment illustrated a **higher**
305**number of apoptotic cells as compared to the control, as shown in Fig. 6A, B.**

3063.9.^[59] Gene expression

307Gene expression **was performed in order to detect the effect of** NPs on cells at the gene
308level.^[59] The cDNA for specific apoptotic genes was synthesized after **cells were seeded** and
309exposed to NPs. The RT-PCR data were analyzed using the relative gene expression (Ct)
310method.^[65] Thus, **the data was** given as the fold change in gene expression adjusted to the

311endogenous reference GAPDH gene (Fig. 7A, B, C, and D).^[61] The fold change in the level
312of target genes between treated and untreated cells is represented in Fig. 7A, B, C, and D.
313^[59] The bax gene expression in cells treated with 17 µg/ml was increased 1.5-fold^[53]
314significantly compared to control in cells (Fig. 7A).^[56] Furthermore, at the caspase-3 gene
315level, there is an increase in fold change mRNA expression of most of the WCoNPs
316concentrations, for instance, a significant increase at 11 and 17 µg/ml of WCoNPs (Fig.
3177C).^[50] Moreover, the BCL2 gene, which is considered one of the apoptotic factors, was
318expressed with significant decrease at 11 and 17 µg/ml of WCoNPs (Fig. 7B). While
319p53 gene expression is significantly increasing at all concentrations of NPS in the
320HUVECs cells (Fig. 7D),

321 4. Discussion

322Biological systems are frequently exposed to excessive reactive oxygen species, causing
323a disturbance in the cells natural antioxidant defense systems and resulting in damage to
324all biomolecules, including nucleic acids.^[62] Because of its numerous scientific and
325technological uses, nanotechnology is one of the newest technologies in creative
326research.^[62] Humans are not aware of the increased risk of exposure to nanoparticles, which
327can enter biological systems through many routes, which is a significant and concurrent
328consequence of these growing nano-based applications.^[62] In instance, nanoparticles can
329morph in size over a range of mediums and offer a measurable increase in surface area in
330comparison to mass.^[89] One of the most often utilized models for endothelial cells in vitro is
331the human umbilical vein endothelial cells (HUVECs) (Garbern et al., 2013). In the
332current study examined the harmful effects of NPs on HUVECs cells, the processes

333behind these effects, and the interactions between quercetin and NPs using HUVECs as a
334model. For in vitro research, stem cells constitute a cutting-edge modeling method.^[92] The
335HUVECs model can be used to study the physiological and pathological effects of
336different stimuli in both isolated and co-cultured forms with other cell types, such as
337leukocytes and smooth muscle cells, despite being physiologically representative of the
338human vascular endothelium (Maciag et al., 1981).

339Tungsten carbide cobalt nanocomposite (WC-Co NPs) has been chosen for this
340investigation in order to assess its impact on HUVEC growth inhibition, genotoxic
341reactions, oxidative stress, and apoptotic cell death. WC-Co NPs size distribution was
342shown by the results of dynamic light scattering analysis during physical characterization.
343TEM imaging confirmed the calculated average particle size of 45.26 ± 1 nm.^[51] This is
344comparable to the findings of the study by Moche et al. (2014),^[62] which showed that the
345isolated NP size distribution, as determined by TEM images of the suspension of WC-Co
346NPs, varied from 20 to 160 nm, with 67.8% of NP falling between 50 and 90 nm.

347^[54] On the other hand, cells were exposed to WC-Co NPs and two methods (MTT and NRU)
348were used to check for inhibition of cell proliferation.^[54] The mitochondrial dehydrogenase
349enzyme, which is only active in live cells, reduces water-soluble tetrazolium salt into an
350insoluble formazan, which is the basis for the MTT assay (Alarifi et al., 2016).^[64] The MTT
351data shows that there were several disruptions in the metabolic capacities of the cells,
352which led to the suppression of growth. Following WC-Co NP treatment, the MTT assay
353results are consistent with comparable metabolic abnormalities in the mitochondria of
354HUVECs.^[49] After 24 hours of incubation, HUVECs exposed to WC-Co NPs showed a
355substantial reduction in HUVEC survival at 5, 10, 25, 50, 100, and 150 $\mu\text{g/ml}$, with an

356IC50 value of 23.144 µg/ml. In the same vein, the NRU test verified this outcome. In
357order to manage hereditary illnesses, dietary ingredients are employed as a
358chemoprotective method (Selvendiran et al., 2005). Quercetin may be utilized as a
359nutraceutical to provide protection against a number of diseases, according to some
360research. Since quercetin affects glutathione, enzymes, signal transduction pathways, and
361ROS generation, it is useful in the treatment and prevention of human diseases. The most
362widely recognized and developed mechanism for the potential toxicity of nanoparticles
363(NPs) is most likely the nanomaterial-induced oxidative stress.^[57] Curiously, no
364comprehensive investigation integrating real-time monitoring of cell growth,
365cytotoxicity/genotoxicity, internalization of NPs, formation of ROS, and cell cycle
366analysis of many cell lines indicative of putative retention organs has been documented
367for WC-Co NPs to yet.

368^[87] Our findings suggest that oxidative stress is probably the main mechanism of WC-Co
369toxicity, despite the fact that it has been implicated as the toxic mechanism associated
370with other nanomaterials such as titanium dioxide or silica (Sun et al., 2011). This is
371reportedly linked to the cytotoxic effects of NPs on both cancer and normal cells (Paget
372et al., 2015). The cytotoxicity of WC-Co NPs against different cell types was examined
373by Bastian et al. (2009), who also demonstrated cell type differences. Our results, which
374are in line with those of several previous research (Paget et al., 2015), demonstrated that
375the combination of WC and Co forms a particular hazardous entity that produces more
376ROS. According to a different study by Xu et al.^[64] (2019), quercetin exhibits strong
377antioxidant activity by preserving oxidative balance.^[74] Oxidative stress caused by an excess
378of reactive oxygen species (ROS) is often closely linked to oxidative damage to proteins

379and DNA, which is why nanomaterials are often genotoxic.^[70] Also, quercetin slows the
380cell cycle, angiogenesis, apoptosis, and migration of cancer cells (Kashyap et al., 2016).
381According to our findings, the combination of quercetin and WC-Co NPs enhances their
382ability to prevent ROS generation. Comparing the ROS level to the group treated with
383WC-Co NPs, the results demonstrated a considerable reduction in ROS due to the
384percentage of toxicity. In the majority of cell culture models, quercetin has been shown
385by Chen et al. (2004) to display antioxidant and cell-protective properties;^[88] yet, in other
386investigations, QU has been shown to exhibit prooxidant and cytotoxic properties.^[88] The
387effects of WC-Co NPs, quercetin, or their combination on HUVEC cell lines generated a
388significant ($p < 0.05$)^[37] quantitative dose-dependent increase in ROS levels, which was
389further supported by the lipid peroxide activity assay.

390According to the current findings, WC-Co NPs decreased CAT levels, increased ROS
391and LPO levels, and decreased the viability of HUVEC cell lines.^[64] Mitochondrial damage
392can take place either due to ROS generated on the surface of nanomaterials or due to
393physical damage to the mitochondrial membrane. The disturbed oxidant balance can
394occur either through increased ROS production or through a defective antioxidant
395defense in response to persistent nanomaterial exposure (Pathak et al., 2015).^[58] Our results
396are consistent with previous reports that bcl2, mRNA and protein expression levels are
397markedly elevated in apoptotic cells at As_2O_3 dosages that cause apoptosis in BEAS-2B
398cells (Tang et al., 2021). By upregulating the expression of bax, caspase-3, and p53 and
399downregulating the expression of bcl-2, it was clear that WC-Co NPs caused apoptosis in
400HUVEC cells. The anti-inflammatory properties of quercetin may lessen the harmful
401effects of WC-Co NPs.^[59] While WC-Co NPs significantly increased the degree of

402apoptosis induction, we observed that when only exposed cells were compared to the
403control, a higher level of apoptosis induction was observed in high-concentration of WC-
404Co NPs. This was confirmed in this study^[59], particularly for 17µg/ml of WC-Co NPs
405without quercetin.

406^[82] Conclusion

407On the basis of our finding in this experiment we conclude that in the future, new
408anticancer therapies can be developed using different approaches, such as a combination
409of metals targeting multiple cancer cell lines, exploring different in vivo models to reveal
410interlinked signaling pathways, and identifying the potential benefits of WC-Co NPs in
411different cancer types to achieve targeted drug delivery.

412^[86] Declaration of conflicting interests

413None

414 Acknowledgments

415This research was supported by Researchers Supporting Project number (RSP2024R27),
416King Saud University, Riyadh, Saudi Arabia.

417 References

- 418 Akbaba GB, Turkez H, Sönmez E, Tatar A, Yilmaz M. Genotoxicity in primary human
419 peripheral lymphocytes after exposure to lithium titanate nanoparticles in vitro.
420 Toxicology and Industrial Health. 2016;32(8):1423-1429.
- 421 Alarifi, S., Ali, D., & Al-Bishri, W. (2016). In vitro apoptotic and DNA damaging
422 potential of nano barium oxide. International journal of nanomedicine, 11, 249

- 423Ali ,. Ray R.S, Hans R.K., UVA-induced cytotoxicity and DNA damaging potential of
424 benz (e) acephenanthrylene, *Toxicology Letters*, 2010; 199(2):193-200.
- 425Ali D, Verma A., Mujtaba F., Dwivedi A., Hans, R.K Ray R.S., UVB-induced apoptosis
426 and DNA damaging potential of chrysene via reactive oxygen species in human
427 keratinocytes, *Toxicology Letters*, Volume 204, I(2–3),2011, 199-207.
- 428Almutairi B, Ali D, Yaseen KN, Alothman NS, Alyami N, Almukhlafi H, Alakhtani S
429 and Alarifi S (2021) Mechanisms of Apoptotic Cell Death by Stainless Steel
430 Nanoparticle Through Reactive Oxygen Species and Caspase-3 Activities on Human
431 Liver Cells. *Front. Mol. Biosci.* 8:729590.
- 432Arora N, Thangavelu K, Karanikolos G N. Bimetallic Nanoparticles for Antimicrobial
433 Applications. *Front. Chem.*, 2020,8: 2020.
- 434Bastian S, Busch W, Kühnel D, Springer A, Meissner T, Holke R, Scholz S, Iwe M,
435 Pompe W, Gelinsky M, Potthoff A, Richter V, Ikonomidou C, Schirmer K. Toxicity
436 of tungsten carbide and cobalt-doped tungsten carbide nanoparticles in mammalian
437 cells in vitro. *Environ Health Perspect.* 2009 Apr;117(4):530-6.
- 438Cao Y, Gong Y, Liu L, Zhou Y, Fang X, Zhang C, Li Y and Li J. The use of human
439 umbilical vein endothelial cells (HUVECs) as an in vitro model to assess the toxicity
440 of nanoparticles to endothelium: a review. *J. Appl. Toxicol.* 2017; 37: 1359-1369.
- 441Chen, J., Ou, Y.-x., Da, W.-m., & Kang, J.-h. (2004). Coadjustment of quercetin and
442 hydrogen peroxide: the role of ROS in the cytotoxicity of quercetin. *Die Pharmazie-*
443 *An International Journal of Pharmaceutical Sciences*, 59(2), 155-158.

444 Freddy Van Goethem, Dominique Lison, Micheline Kirsch-Volders, Comparative
445 evaluation of the in vitro micronucleus test and the alkaline single cell gel
446 electrophoresis assay for the detection of DNA damaging agents: genotoxic effects
447 of cobalt powder, tungsten carbide and cobalt–tungsten carbide, *Mutation Research/
448 Genetic Toxicology and Environmental Mutagenesis*, Volume 392, Issues 1–
449 2, 1997, Pages 31-43.

450 Kashyap, D., Mittal, S., Sak, K., Singhal, P., & Tuli, H. S. (2016). Molecular mechanisms
451 of action of quercetin in cancer: recent advances. *Tumor Biology*, 37, 12927-12939.

452 Kim E-J, 555 Thanh T L, 5555 Chang Y-S. Comparative toxicity of bimetallic Fe
453 nanoparticles toward *Escherichia coli*: mechanism and environmental implications.
454 *Environ. Sci.: Nano*, 2014, 1, 233.

455 Laila, F., Fardiaz, D., Yuliana, N. D., Damanik, M. R. M., & Nur Annisa Dewi, F.
456 (2020). Methanol Extract of *Coleus amboinicus* (Lour) Exhibited
457 Antiproliferative Activity and Induced Programmed Cell Death in Colon Cancer Cell
458 WiDr. *International Journal of Food Science*, 2020, 9068326.
459 doi:10.1155/2020/9068326

460 Maciag, T.; Hoover, G.A.; Stemerman, M.B.; Weinstein, R. Serial propagation of human
461 endothelial cells in vitro. *J. Cell Biol.* 1981, 591, 420–426.

462 Mirowsky J, Hickey C, Horton L, Blaustein M, Galdanes K, Peltier RE, Chillrud S, Chen
463 LC, Ross J, Nadas A, Lippmann M, Gordon T. The effect of particle size, location
464 and season on the toxicity of urban and rural particulate matter. *Inhal Toxicol.*
465 2013;25(13):747-57.

466Mossman, T. (1983). Rapid colorimetric assay for cellular growth and survival:
467 application to proliferation and cytotoxicity assays. *J. Immunol. Methods*, 65, 55.

468Paget, V., Moche, H., Kortulewski, T., Grall, R., Irbah, L., Nesslany, F., & Chevillard, S.
469 (2015). Human cell line-dependent WC-Co nanoparticle cytotoxicity and
470 genotoxicity: a key role of ROS production. *Toxicological Sciences*, 143(2), 385-
471 397.

472Pathak, R. K., Kolishetti, N., & Dhar, S. (2015). Targeted nanoparticles in mitochondrial
473 medicine. *Wiley Interdisciplinary Reviews: Nanomedicine and Nanobiotechnology*,
474 7(3), 315-329.

475Selvendiran K., Thirunavukkarasu C., Singh J. P., Padmavathi R., Sakthisekaran D.
476 (2005). Chemopreventive effect of piperine on mitochondrial TCA cycle and phase-I
477 and glutathione-metabolizing enzymes in benzo(a)pyrene induced lung
478 carcinogenesis in Swiss albino mice. *Mol. Cell. Biochem.* 271, 101–106.

479Setyawati MI, Tay CY, Docter D, Stauber RH, Leong DT. 2015. Understanding and
480 exploiting nanoparticles' intimacy with the blood vessel and blood. *Chem. Soc. Rev.*
481 44: 8174–8199.

482Sun, L., Li, Y., Liu, X., Jin, M., Zhang, L., Du, Z, Sun, Z. (2011). Cytotoxicity and
483 mitochondrial damage caused by silica nanoparticles. *Toxicology in Vitro*, 25(8),
484 1619-1629.

485Tang, J., Yao, C., Liu, Y., Yuan, J., Wu, L., Hosoi, K., . . . Chen, G. (2021). Arsenic
486 trioxide induces expression of BCL-2 expression via NF-κB and p38 MAPK

487 signaling pathways in BEAS-2B cells during apoptosis. *Ecotoxicology and*
488 *Environmental Safety*, 222, 112531.

489 Xu M, et al (2019). Quercetin inhibits angiogenesis mediated human prostate tumor
490 growth by targeting VEGFR-2 regulated AKT/mTOR/P70S6K signaling pathways.
491 *PLoS One*, 7, e47516.